IEEE Photonics Journal
An IEEE Photonics Society Publication

Open Access

Double-Slit and Square-Slit Interferences With Surface Plasmon Polaritons Modulated by Orbital Angular Momentum Beams

Volume 7, Number 2, April 2015

Hailong Zhou
Yifeng Zhou
Jihua Zhang
Jianji Dong

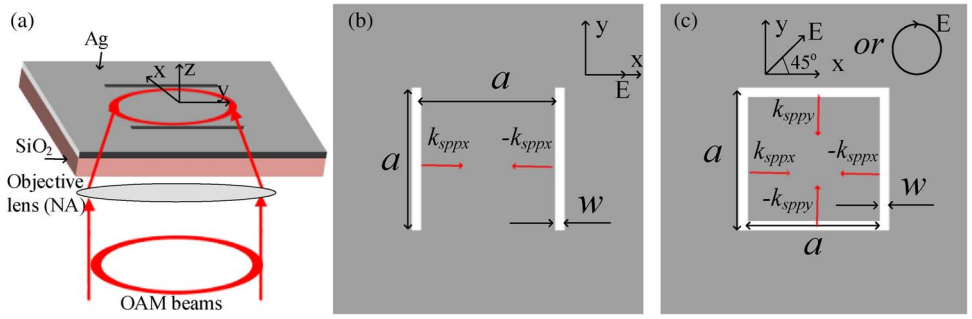

DOI: 10.1109/JPHOT.2015.2415671
1943-0655 © 2015 IEEE

IEEE photonics SOCIETY

IEEE

Double-Slit and Square-Slit Interferences With Surface Plasmon Polaritons Modulated by Orbital Angular Momentum Beams

Hailong Zhou, Yifeng Zhou, Jihua Zhang, and Jianji Dong

Wuhan National Laboratory for Optoelectronics, School of Optoelectronic Science and Engineering, Huazhong University of Science and Technology, Wuhan 430074, China

DOI: 10.1109/JPHOT.2015.2415671

Manuscript received January 16, 2015; revised March 11, 2015; accepted March 12, 2015. Date of publication March 20, 2015; date of current version April 1, 2015. This work was supported in part by the National Basic Research Program of China under Grant 2011CB301704, by the Program for New Century Excellent Talents in Ministry of Education of China under Grant NCET-11-0168, by the Foundation for the Author of National Excellent Doctoral Dissertation of China under Grant 201139, and by the National Natural Science Foundation of China under Grant 11174096 and Grant 61475052. Corresponding author: J. Dong (e-mail: jjdong@mail.hust.edu.cn).

Abstract: We present two kinds of interferences on metallic thin films with orbital angular momentum (OAM) beams, namely, double-slit interference and square-slit interference. When an OAM beam is normally incident upon the metallic thin film with two slits, the fringes on the metallic thin film generated by the interference of two surface-plasmon-polariton waves will twist, and the twist amount depends on the topological charge of the incoming OAM beam. When a square slit is employed, a quasi-square optical lattice will be unveiled, and the arrangement of lattice can be modulated by the OAM beam. The fringes and spots are both at the subwavelength level, which show great potential for superresolution microscopy, OAM detection, and spot-array generation.

Index Terms: Orbital angular momentum, surface plasmon, interferometry.

1. Introduction

Light beams carrying orbital angular momentum (OAM) are associated with an azimuthal phase structure $\exp(il\theta)$, where θ is the angular coordinate, and l is the azimuthal index, defining the topological charge (TC) of the OAM beams [1]. These beams have an OAM of $l\hbar$ per photon ($\hbar$ is Planck's constant h divided by 2π). In recent years, OAM beams have been widely used in many interesting applications, such as optical microscopy [2], micromanipulation [3], quantum information [4], free-space, and fiber optical communication [5]. OAM beams have also been studied in interaction with metallic thin film, such as manipulation of surface plasmon polaritons (SPPs) [6], [7]. SPPs are electromagnetic modes constituted by a light field coupled to a collective electron oscillation propagating along an interface between a metal and a dielectric. Utilizing SPP wave, the traditional interferences can be realized on 2-D micro-scale metallic thin film and the interference patterns can be manipulated by the illuminating OAM beams. In our previous work, we put forward a double-slit interference device based on two metal subwavelength slit arrays to measure the OAM and the polarization of beams simultaneously [8]. However, the

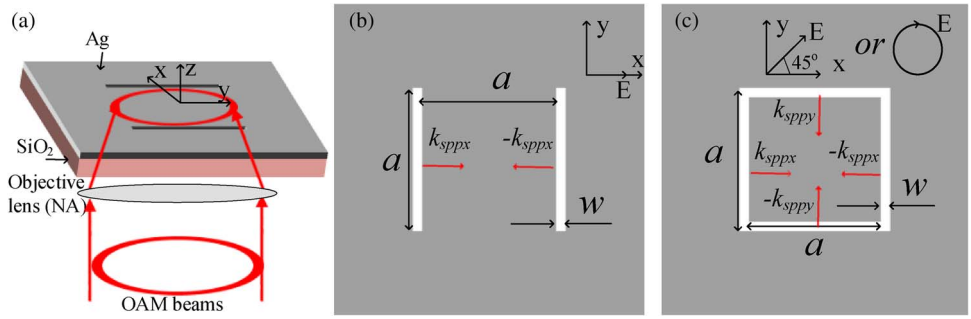

Fig. 1. (a) Schematic structure of the double-slit interference device. (b) Top-view of double-slit interference device. (c) Top-view of square-slit interference device.

interference pattern should be observed on the receiving screen after the double-slit plane. Besides, the interference pattern is larger than wavelength-scale.

In this paper, we present two kinds of interferences on metallic thin films with OAM beams, namely double-slit interference and square-slit interference. Every straight slit can excite an SPP wave. When an OAM beam is normally incident upon the metallic thin film with two slits, the fringes on the metallic thin film generated by the interference of two SPP waves will twist, and the twist amount depends on the TC of the incoming OAM beam. When a square-slit is employed, a quasi-square optical lattice will be unveiled and the arrangement of lattice can be modulated by the OAM beam. The two kinds of interferences indicate that the traditional interferences can also be realized on 2-D micro-sized metallic thin film and show great potential for super-resolution microscopy [9], [10], OAM detection [8], [11]–[13], and spot array generation [14], [15].

2. Principle and Structure

Fig. 1(a) and (b) present the schematic structure and geometric parameters of the double-slit interference device. Similar to [16], we design two slits in a metal (silver) film with a thickness of 120 nm and the metal film is deposited on the silica substrate. The spacing between the two slits and the length of the slits are both $a = 20$ μm. The slit width is $w = 200$ nm. The permittivity of the silver can be described by the Drude model $\varepsilon_m(\omega) = \varepsilon_\infty - \omega_p^2/[\omega(\omega + i\gamma_c)]$, where $\varepsilon_\infty = 6$ is the bulk permittivity at infinite frequency, $\omega_p = 1.5 \times 10^{16}$ rad/s and $\gamma_c = 7.73 \times 10^{13}$ rad/s are the plasma frequency and the collision frequency, respectively [17]. In this case, the intensity distribution in the middle area of the metallic thin film is mainly from the interference of the two SPP waves shown in Fig. 1(b). When a square-slit is employed, the parameters shown in Fig. 1(c) are the same with those in Fig. 1(b). And the intensity distribution in the middle area is mainly from the interference of the four SPP waves shown in Fig. 1(c).

To ensure the maximum excitation efficiency of SPPs, an OAM beam polarized along the x direction and focused by an objective lens normally illuminates the metallic film with two slits. The OAM beams can be produced by passing a plane wave through an azimuthally modulated phase mask or a spatial light modulator [18]. Assume that the focused beam, which illuminates the metallic film, is an ordinary Gaussian vortex beam, which is expressed as

$$E_{in1}(r, \theta) = (r/w)^{|l|} \exp(-r^2/w^2) \exp(il\theta) \tag{1}$$

where (r, θ) are 2-D polar coordinates corresponding to rectangular coordinates (x, y). We assume that the radius of the OAM beam $(w\sqrt{l/2})$, which illuminates the metallic thin film, equals $a/2$, to ensure the best coupling efficiency of SPP wave and a flat intensity distribution in the silts. The wavelength is set as 633 nm, resulting in the corresponding SPP wavelength of $\lambda_{sp} =$ 617 nm and propagation length of 53 um. Similar to the analytical method in [8], we only need consider the interference along the x direction because the y-component of wavevector (k_{sppy})

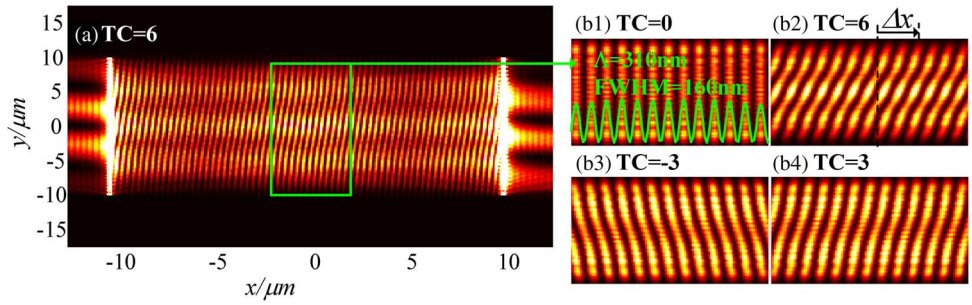

Fig. 2. (a) Overall view and (b1)–(b4) zoom in (size, 4 μ m $\times$ 20 μm) of the interference fringes with different TCs.

is much smaller than the x-component of wavevector (k_{sppx}). Thereafter, the SPP waves in opposite directions shown in Fig. 1(b) will interfere in the middle area. Set the coordinate origin as the center of schematic structure, we call the phase along the left slit $\phi_1(y)$ and the phase along the right slit $\phi_2(y)$. The additional phase difference between the two diffraction-slits along the y-axis can be deduced by

$$\delta\phi(y) = \phi_1(y) - \phi_2(y) = -l\pi - 2l\arctan\frac{2y}{a}. \tag{2}$$

The intensity distribution of interference pattern between two slits is given by

$$I(x, y) \propto \cos^2[k_{sppx}x + \delta\phi(y)/2]. \tag{3}$$

From (3), it can be derived that the fringe space is

$$\Lambda = \pi/k_{sppx}. \tag{4}$$

The fringes are displayed as an equidistantly linear array. The trace of central fringe (bright for even TC and dark for odd TC) can be described as

$$x = \frac{l\Lambda}{\pi}\arctan\frac{2y}{a}. \tag{5}$$

From (5), one can see that when y/a changes from -0.5 to 0.5, x changes value from $x_- = -\Lambda l/4$ to $x_+ = \Lambda l/4$. This means that the fringes twist. We define the twist amount as $\Delta x = x_+ - x_- = \Lambda l/2$, which is proportion to |TC| and the direction of twist is dependent on the sign of TC.

When a metallic thin film with square slits is employed, an OAM beam polarized along the 45° direction with the x axis or a circularly polarized OAM light normally illuminates the metallic thin film, it can be regarded as the superposition of the two sets of double-slit interference fringes with a fixed phase difference. It can be inferred that a quasi-square optical lattice will be unveiled and will incline when changing the TC of the incoming OAM beam.

3. Simulation Results and Analysis

Assume that an OAM beam polarized along the x direction normally illuminates the metallic thin film with two slits. We calculate the interference patterns for different OAM beams illuminating through 3-D finite difference time domain (FDTD) simulations. Fig. 2(a) presents the overall view of the interference patterns of the SPP waves when TC = 6, and Fig. 2(b1)–(b4) presents the zoom in of interference patterns at the center when different OAM beams illuminate, the pattern size is 4 μm $\times$ 20 μm. Because the transmittance is very low and the intensity of the input OAM beam is annular, the OAM beam almost does not interfere with the SPPs in the interfered region, and the simulations also prove the inference. The green solid line in Fig. 2(b1) shows

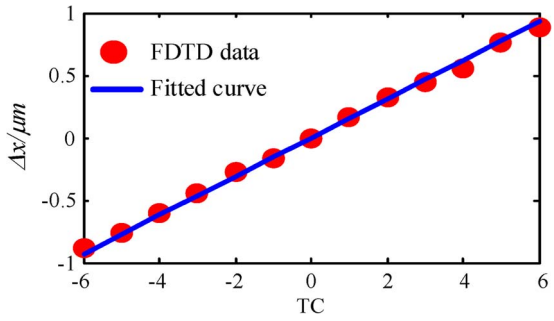

Fig. 3. Twist amount of the fringes dependence on TC.

the intensity distribution in cross-section view when TC $= 0$. The fringe spacing Λ is approximately equal to 310 nm, and the full width at half maximum (FWHM) of every fringe is about 160 nm. One can see that the fringes are straight and parallel each other when the TC equals zero, which is similar to the conventional Young's double-slit interference. When we change the TC of the incoming OAM beam, the fringes will twist, as shown in Fig. 2(b2)–(b4). The twist direction is opposite when changing the sign of the TC such as the cases where the TCs $= 3$ or -3 in Fig. 2(b3) and (b4). And the twist amount will increase as the absolute value of TC increases, as shown in Fig. 2(b1), (b2), and (b4).

The simulation results agreed well with the abovementioned analysis. We have concluded that, the interference fringes will twist, and the twist amount of interference patterns depend on the TC of OAM beams. Fig. 3 shows the measured twist amount as a function of TC, as shown with the red dots. And the blue solid line is the linearly fitted curve for comparison. One can see that the twist amount is nearly proportional to TC. In particular, the slope of the fitted curve is about 155 nm which is equal to $\Lambda/2$, it agrees well with the abovementioned analysis, where $\Delta x = \Lambda l/2$. The measurement errors mainly come from the cases where an OAM beam with a large TC illuminates. It may be caused by that the model in (3)–(5) has slight errors when TCs are large, but it is still accurate enough. In addition, from Fig. 2(a), one can see that the interference appears in y direction with a large period of about 5.4 μm, which is caused by the small y-component of wavevector (k_{sppy}). In the analysis, the y-component of wavevector (k_{sppy}) is ignored in (3), but it will increase when |TC| increases, which results in an observable interference in y direction. In particular, the k_{sppy} will be zero and the period in y direction becomes infinite when TC equals 0. In this case, the interference in y direction will disappear and the fringe spacing in x direction is measured to be 310 nm in the simulation, which matches well with the theoretical calculation of $\lambda_{sp}/2$. The error is caused by the mesh accuracy (setting with 10 nm) in x direction, so it is reasonable that the measured value deviates with several nanometers.

In fact, the linear model has a large alignment tolerance. Assume that the two slits are expressed as $x = x_1, x = x_2 (x_2 - x_1 = a)$, respectively, so we can deduce that

$$\delta\phi(y) = l\arctan\frac{y}{x_1} - l\arctan\frac{y}{x_2} + c_1 \tag{6}$$

where c_1 is a constant. We can see that $\delta\phi(y)$ still linearly depends on l, so Δx is still proportional to l. It means that the results are not sensitive to the geometrical alignment between the OAM beam and the sample, and therefore, it has a large alignment tolerance. But the central deviation cannot be too large, because it will make the input intensity in the slits dramatically vary along the y direction, thus the interference fringes have a corresponding intensity modulation in the y direction, which will affect the interference effect.

A metallic thin film with two slits can generate an interference pattern of the SPP waves with parallel fringes. It can be inferred that a quasi-square optical lattice will be unveiled when a metallic thin film with square slits is employed. Fig. 4 displays the interference patterns when

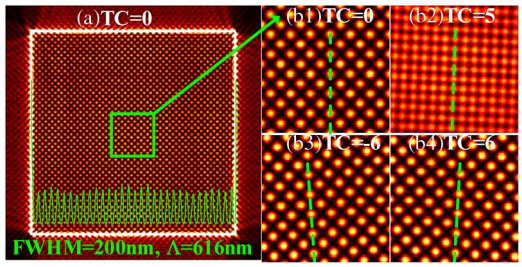

Fig. 4. Optical lattice generated by the square-slit interference when 45° polarized OAM beams illuminate.

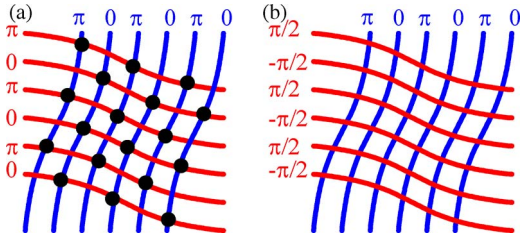

Fig. 5. Superposition of the intensity of the two double-slit interference by 45° polarized OAM beams illuminating when (a) TC is even and (b) TC is odd.

different OAM beams polarized along the 45° direction with the *x* axis normally illuminate the metallic thin film. One can see that a square optical lattice is generated clearly when TC equals 0, as shown in Fig. 4(a). The green solid line shows the intensity distribution along the cross section of one row of the spot array. The spot spacing Λ is approximately equal to 616 nm, and the FWHM of every spot is about 200 nm. Fig. 4(b1)–(b4) present the zoom in of interference patterns at the center when different OAM beams illuminate, the pattern size is 4 μm $\times$ 4 μm. When we change the incoming OAM beam, the optical lattice will incline, the inclined direction depends on the sign of TC and the inclined amount increases with the |TC|, shown as the green dotted line in Fig. 4(b1)–(b4). We also notice that the bright spot array is very legible when TC is even but fuzzy when TC is odd. In turn, the dark spot array is fuzzy when TC is even but legible when TC is odd. In addition, the period become 309 nm (approximately half of 616 nm) when TC is odd.

All the above phenomena can be explained with the superposition of the intensity of the two double-slit interference, as shown Fig. 5. The blue lines (column) are the bright fringes caused by the vertical double-slit and the red set (row) are the bright fringes caused by the horizontal double-slit. It can be inferred that the phase difference between the adjacent fringes is π due to the opposite directions of the two SPP waves. The two pairs of double-slit are placed perpendicularly, so the phase difference between the two sets of interference fringes is $\pi/2$. That is, the phase difference equals to 0 or π when the TC of the incoming OAM beam is even and $\pm\pi/2$ when TC is odd. When the TC is even, some intersections of twist fringes have the same phase which results in enhanced superposition (black filled circles) and their adjacent intersections have a phase difference of π which leads to destructive superposition, as shown in Fig. 5(a). Therefore the bright spots are very legible and the spot spacing (616 nm) is approximately two times of the fringe spacing (310 nm) as shown in Fig. 4(a), (b1), (b3), and (b4). When TC is odd as shown in Fig. 5(b), the phase difference between the two sets of interference fringes is $\pm\pi/2$. This means the intersections are always partial constructive (the intensity become $|1 \pm i|^2$ times), so the bright spots become blurry, the black spots become legible and the period become half of Λ, as shown in Fig. 4(b2). In addition, the spot array will incline with the twist fringes. And the FWHM of the spots is slightly larger than that of the twist fringes in double-slit case due to the superposition of the fringes from two orthogonal directions.

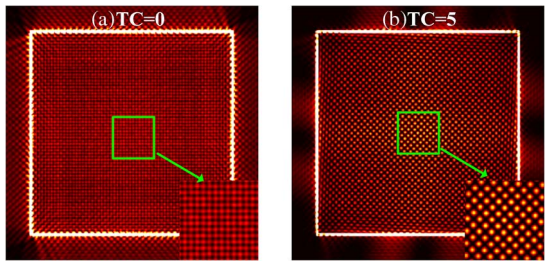

Fig. 6. Optical lattice generated by the square-slit interference when a circularly polarized OAM light is normally incident on the metallic thin film.

Besides, we can infer that the sharpness of optical lattice will be reversed when a circularly-polarized OAM light is normally incident on the metallic thin film owing to the contribution of extra phase difference of $\pi/2$ between *x* and *y* directions. Fig. 6 shows the comparison of optical lattice when TC is even and odd. The bright spot is blurry when the TC is even and becomes very legible when the TC is odd. In addition from Fig. 6(b), one notices that the interference appears outside the square slits, which is also caused by SPP wavevectors parallel to the corresponding silts. The periods will increase when decreasing the |TC|. Especially, the period parallel to the silts becomes infinite when TC equals 0 shown in Fig. 4(a) and Fig. 6(a), which is similar to the case of double-slit interference in y direction, as shown in Fig. 2(a).

There are many potential applications of the two kinds of interferences. The double-slit interference patterns are equidistant fringes. The fringes will twist and the twist amount related to the TC of the incoming OAM beam is linear; therefore, it reveals an alternative to detect the OAM of light [8], [11]–[13], which is shown in Fig. 3. Comparing to our previous method in free space interference [8], this method offers an interference pattern on the metallic film directly without an extra receiving screen. Besides, the twist pattern is subwavelength scale to offer compact size, and it offers a method to modulate the interference fringes of the SPP waves as well [7]. The 1-D fringes have a FWHM of 160 nm and a period of 310 nm, which shows great potential for super-resolution microscopy [9], [10]. The 2-D and super-resolution optical lattice [14], [15] can also be generated by employing square slits. The spot array can be designed to be very sharp with a FWHM of 200 nm and a period of 616 nm, which can be also applied in 2-D super-resolution microscopy, and OAM detection as well. In terms of detecting OAM TC, the optical lattice offers two parallel measurements due to 2-D structure. This may reduce the measurement errors to some extent.

4. Conclusions

In conclusion, we have presented two kinds of interferences on metallic thin films with OAM beams, namely, double-slit interference and square-slit interference. When an OAM beam is normally incident upon the metallic thin film with two slits, the fringes on the metallic thin film generated by the interference of two SPP waves will twist, and the twist amount depends on the TC of the incoming OAM beam. When a square-slit is employed, a quasi-square optical lattice will be unveiled and the arrangement of lattice can be modulated by the OAM beam. Our methods indicate that the traditional interferences can also be realized on 2-D micro-sized metallic thin film. In addition, the fringes and spots are both subwavelength scale, which show great potential for super-resolution microscopy, OAM detection, and spot array generation.

References

[1] L. Allen, M. Beijersbergen, R. Spreeuw, and J. Woerdman, "Orbital angular momentum of light and the transformation of Laguerre-Gaussian laser modes," *Phys. Rev. A*, vol. 45, pp. 8185–8189, 1992.
[2] S. Fürhapter, A. Jesacher, S. Bernet, and M. Ritsch-Marte, "Spiral interferometry," *Opt. Lett.*, vol. 30, pp. 1953–1955, Aug. 1, 2005.

[3] D. G. Grier, "A revolution in optical manipulation," *Nature*, vol. 424, pp. 810–816, 2003.
[4] A. Mair, A. Vaziri, G. Weihs, and A. Zeilinger, "Entanglement of the orbital angular momentum states of photons," *Nature*, vol. 412, pp. 313–316, 2001.
[5] N. Bozinovic *et al.*, "Terabit-scale orbital angular momentum mode division multiplexing in fibers," *Science*, vol. 340, pp. 1545–1548, 2013.
[6] A. Liu, G. Rui, X. Ren, Q. Zhan, G. Guo, and G. Guo, "Encoding photonic angular momentum information onto surface plasmon polaritons with plasmonic lens," *Opt. Exp.*, vol. 20, pp. 24 151–24 159, Oct. 22, 2012.
[7] G. H. Yuan, X. C. Yuan, J. Bu, P. S. Tan, and Q. Wang, "Manipulation of surface plasmon polaritons by phase modulation of incident light," *Opt. Exp.*, vol. 19, pp. 224–229, Jan. 1, 2011.
[8] H. Zhou, S. Yan, J. Dong, and X. Zhang, "Double metal subwavelength slit arrays interference to measure the orbital angular momentum and the polarization of light," *Opt. Lett.*, vol. 39, pp. 3173–3176, Jun. 1, 2014.
[9] P. Tan, X.-C. Yuan, G. Yuan, and Q. Wang, "High-resolution wide-field standing-wave surface plasmon resonance fluorescence microscopy with optical vortices," *Appl. Phys. Lett.*, vol. 97, 2010, Art. ID. 241109.
[10] E. Chung, Y.-H. Kim, W. T. Tang, C. J. Sheppard, and P. T. So, "Wide-field extended-resolution fluorescence microscopy with standing surface-plasmon-resonance waves," *Opt. Lett.*, vol. 34, pp. 2366–2368, 2009.
[11] P. H. F. Mesquita, A. J. Jesus-Silva, E. J. S. Fonseca, and J. M. Hickmann, "Engineering a square truncated lattice with light's orbital angular momentum," *Opt. Exp.*, vol. 19, pp. 20616–20621, Oct. 10, 2011.
[12] J. Hickmann, E. Fonseca, W. Soares, and S. Chávez-Cerda, "Unveiling a truncated optical lattice associated with a triangular aperture using light's orbital angular momentum," *Phys. Rev. Lett.*, vol. 105, 2010, Art. ID. 053904.
[13] J. G. Silva, A. J. Jesus-Silva, M. A. R. C. Alencar, J. M. Hickmann, and E. J. S. Fonseca, "Unveiling square and triangular optical lattices: A comparative study," *Opt. Lett.*, vol. 39, pp. 949–952, Feb. 15, 2014.
[14] D. Cojoc *et al.*, "Phase diffractive elements for three dimensional spot arrays generation," in *Proc. Int. CAS*, vol. 1, 2001, pp. 217–220.
[15] M. Ghisoni, J. Bengtsson, J. Vukusic, H. Martinsson, and A. Larsson, "Single- and multimode VCSELs operating with continuous relief kinoform for focussed spot-array generation," *IEEE Photon. Technol. Lett.*, vol. 9, pp. 1466–1468, Nov. 1997.
[16] S. Wei *et al.*, "Singular diffraction-free surface plasmon beams generated by overlapping phase-shifted sources," *Opt. Lett.*, vol. 38, pp. 1182–1184, Apr. 1, 2013.
[17] J. Sun, J. Zeng, and N. M. Litchinitser, "Twisting light with hyperbolic metamaterials," *Opt. Exp.*, vol. 21, pp. 14 975–14 981, Jun. 17, 2013.
[18] G. Lazarev, A. Hermerschmidt, S. Krüger, and S. Osten, "LCOS spatial light modulators: Trends and applications," *Optical Imaging and Metrology: Advanced Technologies*, W. Osten and N. Reingand Eds. Weinheim, Germany: Wiley-VCH Verlag, 2012.